Exploration of C-Band σ^o Dependence on Azimuth Angle over Antarctic Sea and Glacial Ice

David S. Early and David G. Long

Brigham Young University Electrical and Computer Engineering Department
459 Clyde Building, Provo, UT 84602
earlyd@newt.ee.byu.edu long@ee.byu.edu Fax: (801) 378-6586

Abstract - **In previous studies, the radar backscatter measurements from polar glacial ice have demonstrated modulation in azimuth angle. Azimuthal modulation is a function of the wind induced surface characteristics of the glacial ice. In a continuing evaluation of the ERS1 C-band scatterometer as a tool for studying polar sea ice, we evaluate the azimuthal modulation characteristics of Antarctic sea ice. Using several study regions dispersed in the Antarctic seasonal sea ice pack, the scatterometer data is evaluated for evidence of azimuthal modulation. The incidence angle dependence is estimated and removed in each study region before determining whether azimuthal modulation is present in the data. Our results show that there is negligible azimuthal modulation at the scale of observation of the ERS1 C-band scatterometer.**

I. INTRODUCTION

In this paper, we address the issue of azimuthal modulation of the microwave signature over Southern Hemisphere sea ice and Antarctic glacial ice in ERS-1 C-band scatterometer data. Our primary interest in this study is in the polar sea ice azimuthal modulation characteristics. Glacial ice is studied for comparison since azimuthal modulation has been observed over Antarctic glacial ice using the Seasat Ku-band scatterometer [1].

The paper is organized into two sections. The first addresses the selection and processing of the ERS-1 data. The second draws conclusions from the data plots and assesses the presence of azimuthal modulation.

II. PROCEDURE

For this study, several study regions encompassing Antarctic sea ice and glacial ice are selected. The regions are chosen to ensure a homogeneous surface response and good azimuthal diversity. The data is corrected for incidence angle dependence and plots of σ^o vs. azimuth angle are made to evaluate azimuthal modulation.

Study Regions

Study regions are chosen based on the assumption that the surface in the region is homogeneous. To aid in the selection of homogeneous regions, we use enhanced resolution images of Antarctic glacial and sea ice. The spatial homogeneity of the σ^o measurements in a study region reduces the variance of the measurements, ensuring accurate assessment of low level (1 dB) azimuthal modulation. Examples of enhanced resolution images can be found in [2], and an explanation of the SIRF algorithm for generating the enhanced resolution images is found in [3].

An additional criterion for selecting viable study regions is adequate diversity of azimuth angles. Azimuth diversity is required in order to properly evaluate azimuthal modulation. Azimuth diversity is affected by the size of a study regions and the number of days in the study period. The dynamic nature of the Antarctic sea ice increases the probability that the surface changes over the course of several days. Since several days of data are required to give good azimuthal diversity, temporal homogeneity of the surface is required when selecting study regions.

The successful tradeoff between study region size and the number of days in the data set can be evaluated by visually examining the data. An evaluation of each study region is made to determine whether the data is spatially and temporally homogeneous and whether it has sufficient azimuthal angle diversity to show azimuthal modulation. The evaluation for homogeneity is done by plotting the σ^o values versus incidence angle and evaluating the data visually for σ^o spread and variance in the σ^o vs. incidence angle plot.

To evaluate the data for azimuthal angle diversity, a histogram of azimuth angles for several incidence angle ranges is plotted. An example azimuth angle histogram of ERS-1 scatterometer data over Antarctic sea ice is given in Figure 1 for the incidence angle range 40 to 45 degrees. The reasons for relating azimuthal angle diversity to small incidence angle ranges is discussed in the next section. The ERS-1 data over sea ice shows a limited range of azimuth angles. Notice the groupings of azimuthal angles in the example histogram in Figure 1. These groupings are evident in all the data used in this study and are a consequence of the instrument geometry. Also, due to instrument geometry, very few readings are made at azimuthal angles above 270 degrees or below 90 degrees.

As will be explained in the next section, small incidence angle ranges are used when evaluating azimuthal modulation. Histograms for each incidence angle range are evaluated for each study region for adequate azimuthal diversity. The incidence angle ranges examined in this study are 25° to 30°, 30° to 35°, 35° to 40°, 40° to 45°, 45° to 50°, and 50° to 55°. Two additional ranges near 40°, 37° to 39° and 40° to 42° are used.

After making the evaluations, we found that most regions selected using the enhanced resolution images had a relatively small σ^o spread in each incidence angle range. The incidence angle ranges near 40° exhibit good azimuthal diversity but ranges near the incidence angle extremes are much less likely to have a diversity of azimuthal measurements. A total of 34 study regions are selected and used in this study with 20 regions on the Antarctic continent and in 14 regions in the seasonal sea ice pack.

Incidence Angle Dependence

Since the radar return may have both incidence and azimuth angle dependence, the separation of any incidence angle dependence from the data is crucial to proper interpretation of azimuthal modulation observed in the plots.

The incidence angle dependence of the backscatter over a narrow incidence angle range is modeled by the linear

This work was supported under a NASA Global Change Research Fellowship and in part by NASA Polar Research Program under Dr. Robert Thomas.

0-7803-2567-2/95 $4.00 © 1995 IEEE

equation

$$\sigma^o_{dB} = \mathcal{A} + \mathcal{B}(\theta - 40^\circ) \quad (1)$$

where σ^o_{dB} is the received backscatter in dB and θ is the incidence angle of the measurement. Although 40^o is used here, the data can be normalized to any incidence angle value. $\mathcal{B}$ represents the slope of the data with respect to the incidence angle θ. An estimate of the parameter $\mathcal{B}$, denoted $\widehat{\mathcal{B}}$, is determined from a linear regression of the σ^o measurements for each study region. With a $\widehat{\mathcal{B}}$ estimated for a given study region, the estimate $\widehat{\mathcal{A}}_i$ for each backscatter measurement σ^o_i in the study region is given by

$$\widehat{\mathcal{A}}_i = \sigma^o_i - \widehat{\mathcal{B}}(\theta - 40^\circ). \quad (2)$$

The resulting $\widehat{\mathcal{A}}_i$ values represent incidence angle normalized backscatter values, i.e. the value of σ^o at $\theta = 40^o$.

$\widehat{\mathcal{B}}$ Error

Note that each σ^o measurement in a study region data set represents a unique backscatter measurement from a single radar footprint. The surface area of the footprint is smaller than the total area in a each study region, so it is reasonable to assume that each σ^o measurement has a unique $\mathcal{B}$ associated with it. Error may be introduced by using a single estimate of the $\mathcal{B}$ parameter to determine the incidence angle normalized backscatter estimates $\mathcal{A}_i$.

Suppose that for a given σ^o measurement, the true value of $\mathcal{A}$, $\mathcal{A}_t$ is given by

$$\mathcal{A}_t = \sigma^o_i - \mathcal{B}_t(\theta - 40^\circ) \quad (3)$$

where $\mathcal{B}_t$ represents the true $\mathcal{B}$ value for the σ^o measurement. If $\widehat{\mathcal{B}}$ is not exactly equal to the true value $\mathcal{B}_t$, the error ϵ in $\mathcal{A}_i$ is given by

$$\epsilon = \mathcal{A}_t - \widehat{\mathcal{A}}_i = (\widehat{\mathcal{B}} - \mathcal{B}_t)(\theta - 40^\circ) \quad (4)$$

We can express $\widehat{\mathcal{B}}$ as $\widehat{\mathcal{B}} = \mathcal{B}_t + \xi$, where ξ represents the difference between the true value $\widehat{\mathcal{B}}_t$ and $\widehat{\mathcal{B}}$. Now let ξ_{max} be the maximum $\mathcal{B}$ error, $\xi_{max} = max(\widehat{\mathcal{B}} - \mathcal{B}_t)$. Then the maximum error in $\widehat{\mathcal{A}}$ is

$$\epsilon_{max} = \pm\xi_{max}(\theta - 40^\circ). \quad (5)$$

In this study, the mean $\mathcal{B}$ is approximately -0.2 with a worst case range of 0.0 to -0.4, making $\xi_{max} = \pm 0.2$. The maximum error in $\mathcal{A}$, ϵ_{max}, is plotted vs. incidence angle as in Figure 2.

The data can be normalized to any incidence angle, so the error introduced by incidence angle correction is minimized by normalizing the data to an incidence angle in the middle of each incidence angle range studied. Note that the graph in Figure 2 shows the worst case error, so we expect the error will be much smaller in practice.

III. RESULTS

Figure 3 shows a representative plot of $\widehat{\mathcal{A}}$vs. azimuth angle for an small incidence angle range over sea ice. Figure 4 shows a representative plot of $\widehat{\mathcal{A}}$vs. azimuth angle for an small incidence angle range over glacial ice. $\widehat{\mathcal{A}}$, the incidence angle normalized σ^o , is plotted. Both plots are representative of the graphs produced in this study for all sea ice and glacial regions. There are no major deviations from these representative plots other than the mean which is a function of θ and differs from region to region.

Incidence Dependence Removal

Figures 5 and 6 show a comparison of $\widehat{\mathcal{A}}$, the incidence angle normalized σ^o , on one plot and σ^o on the other for a given region. Note that a large range of incidence angles (10° to 70°) is used for this evaluation to illustrate the impact of incidence angle removal on azimuthal plots. Due to the coupling of the azimuth and incidence angles, it appears as though there may be azimuthal modulation in the uncorrected data set in Fig. 5. However, with the removal of incidence angle dependence, the apparent azimuthal modulation disappears (Fig. 6). Since the incidence angle and azimuth angle for a given reading are related by the orbital geometry, and we can expect some relation between the incidence angle and the azimuth angle. Thus, the apparent azimuthal modulation in Fig. 5 is not true azimuthal modulation.

To further support this, the plot in Fig. 4 (glacial ice) shows modulation in azimuth even with the removal of incidence dependence. Note that the two plots in Fig. 3 and Fig. 4 are made over a small incidence angle range (3^o). Over this smaller range of incidence angles, we do not expect incidence angle effects to be significant. Comparison of corrected and uncorrected plots over small incidence angle ranges shows little difference, as expected.

Azimuthal Modulation

An examination of the plots in Fig. 3 and Fig. 4 reveals two important results. First, there is significant azimuthal modulation over the glacial regions. This is consistent with the results of [1] for Ku-band Seasat scatterometer data. Second, azimuthal modulation of σ^o is less than 1 dB over sea ice.

Remy et. al. [1] demonstrated that the azimuthal modulation over Antarctic glacial ice was related to the kadabatic winds on the continent and possibly ice slope. The winds cause a rippling in the fern on the glacial ice surface that is evident in satellite data as azimuthal modulation. Sea ice, on the other hand, has much different surface characteristics than glacial ice. Snow on the surface of Antarctic sea ice during most stages of formation tends to be saturated with saline water, reducing the effects of wind shaping on the ice surface. Further, since the sea ice floats on the surface of the ocean, we expect no inherent slope associated with sea ice that would induce azimuthal modulation. Any significant slope in the sea ice must result from ridging or stacking of ice floes. The dynamic nature of the sea ice sheet also causes break up and refreezing of sections of the ice which effectively randomizes small scale ridges and wind-induced ripples that may form on the surface of the sea ice. Over the nominal 50km resolution scale of the ERS-1 scatterometer measurements, relatively small, randomly oriented features are unlikely to contribute significantly to azimuthal modulation in the backscatter return. The size of the footprint effectively averages the small, randomly oriented features so that any azimuthal modulation is negligible.

IV. SUMMARY

A detailed analysis of the ERS-1 scatterometer data reveals that there is not any significant azimuthal modulation evident data over Antarctic sea ice. Azimuthal modulation over sea ice was less than 1 dB at the nominal ERS-1 scatterometer resolution of 50 km. Azimuthal modulation is observed over Antarctic glacial ice which is consistent with the results of other studies.

REFERENCES

[1] F. Remy, Ledroit, and J. Minster, "Katabatic wind intensity and direction over antarctica derived from

scatterometer data," *Geophysical Research Letters*, vol. 19, pp. 1021–1024, 1992.

[2] D. Long, D. Early, and M. Drinkwater, "Enhanced resolution ers-1 scatterometer imaging of southern hemisphere polar ice," *Proceedings of IGARSS*, pp. 156–158, 1994.

[3] D. Long, P. Hardin, and P. Whiting, "Resolution enhancement of spaceborne scatterometer data," *IEEE Transactions on Geoscience and Remote Sensing*, vol. 31, pp. 700–715, 1993.

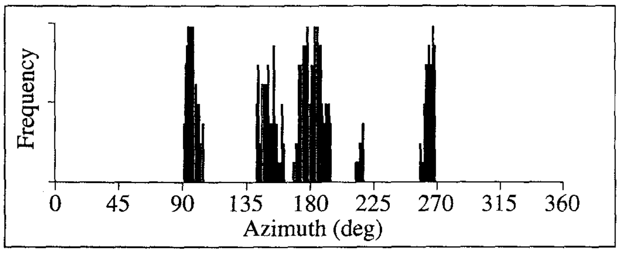

Figure 1. Example histogram of azimuthal angles over Antarctic sea ice. Note the gaps caused by instrument geometry.

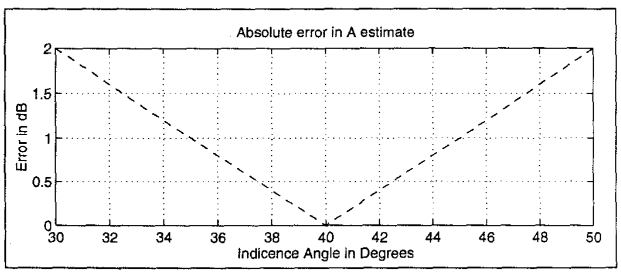

Figure 2. Plot of the maximum error in $\widehat{\mathcal{A}}$ caused by a worst case $\widehat{\mathcal{B}}$error. The error is typically much smaller, on the order of 0.05 dB

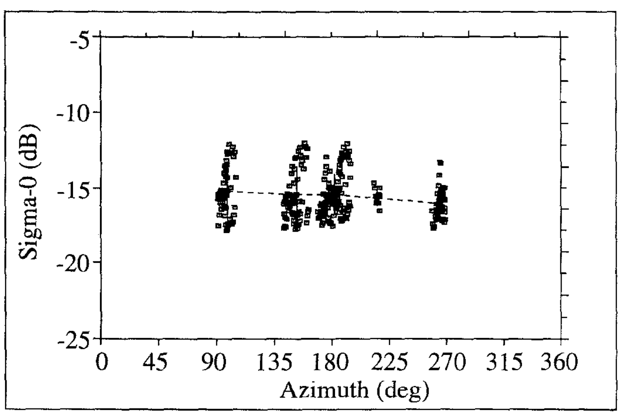

Figure 3. Representative σ^o vs. azimuth angle plot for sea ice. This region is in the Weddell Sea. $\widehat{\mathcal{A}}$, the incidence angle normalized σ^o is plotted.

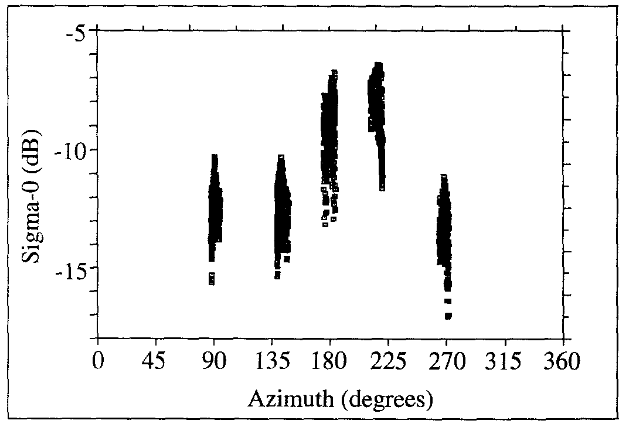

Figure 4. Representative σ^o vs. azimuth angle plot for Antarctic glacial ice. $\widehat{\mathcal{A}}$, the incidence angle normalized σ^o is plotted.

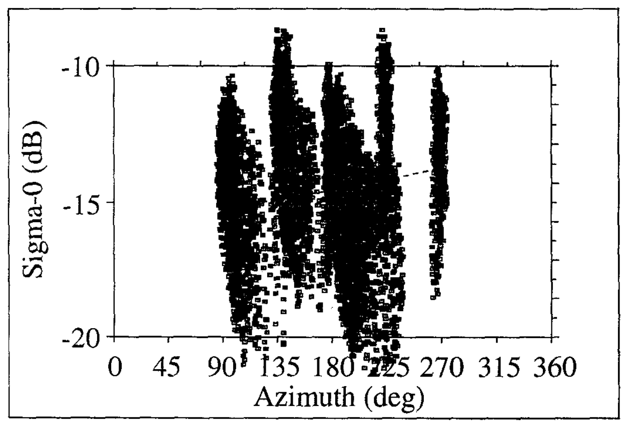

Figure 5. Plot of σ^o vs. azimuth angle, an example of no correction for incidence angle dependencies

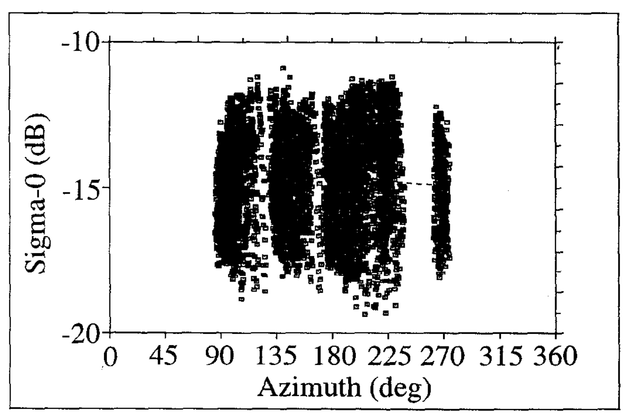

Figure 6. Plot of $\widehat{\mathcal{A}}$ vs. azimuth angle, an example of data with incidence angle dependencies removed.